Acta Cryst. (1955). 8, 530

Growth Features on Crystals of Long-Chain Compounds. I

BY S. AMELINCKX

Laboratorium voor Kristalkunde, Rozier 6, *Gent, Belgium*

(*Received* 8 *February* 1955 *and in revised form* 12 *March* 1955)

A description is given of growth features, observed with phase-contrast microscopy, on crystals of *n*-alcohols ($C_{22}H_{45}OH$, $C_{24}H_{49}OH$ and $C_{26}H_{53}OH$) grown from solutions in benzene and xylene. In this first part special attention is given to interlaced spirals on crystals of the β-form (monoclinic) of the *n*-alcohols. In a second part, growth features observed on crystals of the α-form (orthorhombic) as well as on carboxylic acids will be treated with special reference to imperfect dislocations and to twin growth.

It is shown how the analysis of the growth patterns can lead to unambiguous conclusions concerning the stacking sequence of particular crystals. It is concluded that these crystals exhibit a remarkable polytypism due to spiral growth and to the presence of stacking faults of a well defined type, i.e. relative rotations through angles $\varphi = k \times 60°$ between successive bimolecular layers.

1. Introduction

Electron-microscopic studies of spiral-growth patterns on crystals of long-chain compounds have been made by Dawson *et al.*: *n*-hexatriacontane (Dawson & Vand, 1951), *n*-hectane (Dawson, 1952), *n*-nonatriacontane and stearic acid (Anderson & Dawson, 1953). The growth of stearic and palmitic acid has been investigated by means of phase-contrast microscopy (Verma & Reynolds, 1953). In none of these cases was any reference made either to interlaced spirals or to polytypism. We have studied a series of *n*-carboxylic acids and *n*-alcohols, and we will show in this paper that the crystals of this last series of compounds show a remarkable polytypism, the existence of which can be deduced from the growth patterns alone. Preliminary accounts of these observations have already been published (Amelinckx, 1953*a*, *b*, 1954).

2. Crystallography of the *n*-alcohols

2·1. *Preparation and morphology of crystals*

Crystals are obtained by slow evaporation of a drop of saturated solution on an object glass. The best results were obtained with benzene and xylene as solvents.

The crystals were always small (< 50 microns) lozenge-shaped thin plates, having one face $(00\bar{1})$ in contact with the object glass. The face under observation is $c(001)$; the other faces developed are (110), $(1\bar{1}0)$, $(\bar{1}10)$ and $(\bar{1}\bar{1}0)$.

In the crystallization two polymorphs were always present; they can easily be distinguished by means of the acute angle χ of the lozenge: $\chi = 59°$ and $\chi = 67°$.

Growth features on crystals characterized by $\chi = 59°$ have a line (plane) of symmetry along the long diagonal of the lozenge. Spirals on (001) and $(00\bar{1})$ are turned over 180° about the short diagonal with respect to one another. We can thus conclude that the form $\chi = 59°$ is monoclinic with $b(010)$ perpendicular to the short diagonal; it must be identical with the β-form described by Wilson & Ott (1934).

The form with $\chi = 67°$ should as a consequence be their α-form (orthorhombic), but as only long spacings were published by the authors no direct comparison is possible. It is, however, evident from the correspondence of the angle χ with the one for the orthorhombic form of the paraffins that our conclusion is justified.

2·2. *Crystal structure and stacking possibilities*

No detailed structure determinations are yet published but it is known that *n*-alcohols crystallize in double layers (bimolecular layers) of parallel chains, their polar groups being associated. For the β-form the chains are tilted with respect to (001). From the morphology it is clear that the projection of the chains has the direction of the long diagonal.

As the α-form is orthorhombic, the chains are perpendicular to (001).

The limiting surfaces of a bimolecular layer will consist of CH_3 groups. In the β-form these CH_3 groups are very approximately in a close-packed arrangement, as can be concluded from the special value of χ ($\simeq 60°$). This will have the important consequence that successive bimolecular layers can be stacked in several ways so that 'spheres' fit into 'hollows': (i) We can stack the layers in different ways corresponding to the two different series of hollows available ($\triangle$ and $\triangledown$ hollows) (notation introduced by Frank, 1951). (ii) We can turn successive layers through angles $\varphi = k \times 60°$. This last operation is a symmetry operation for a close-packed layer of spheres, but not for a layer of tilted chains.

In what follows we shall not have to consider the

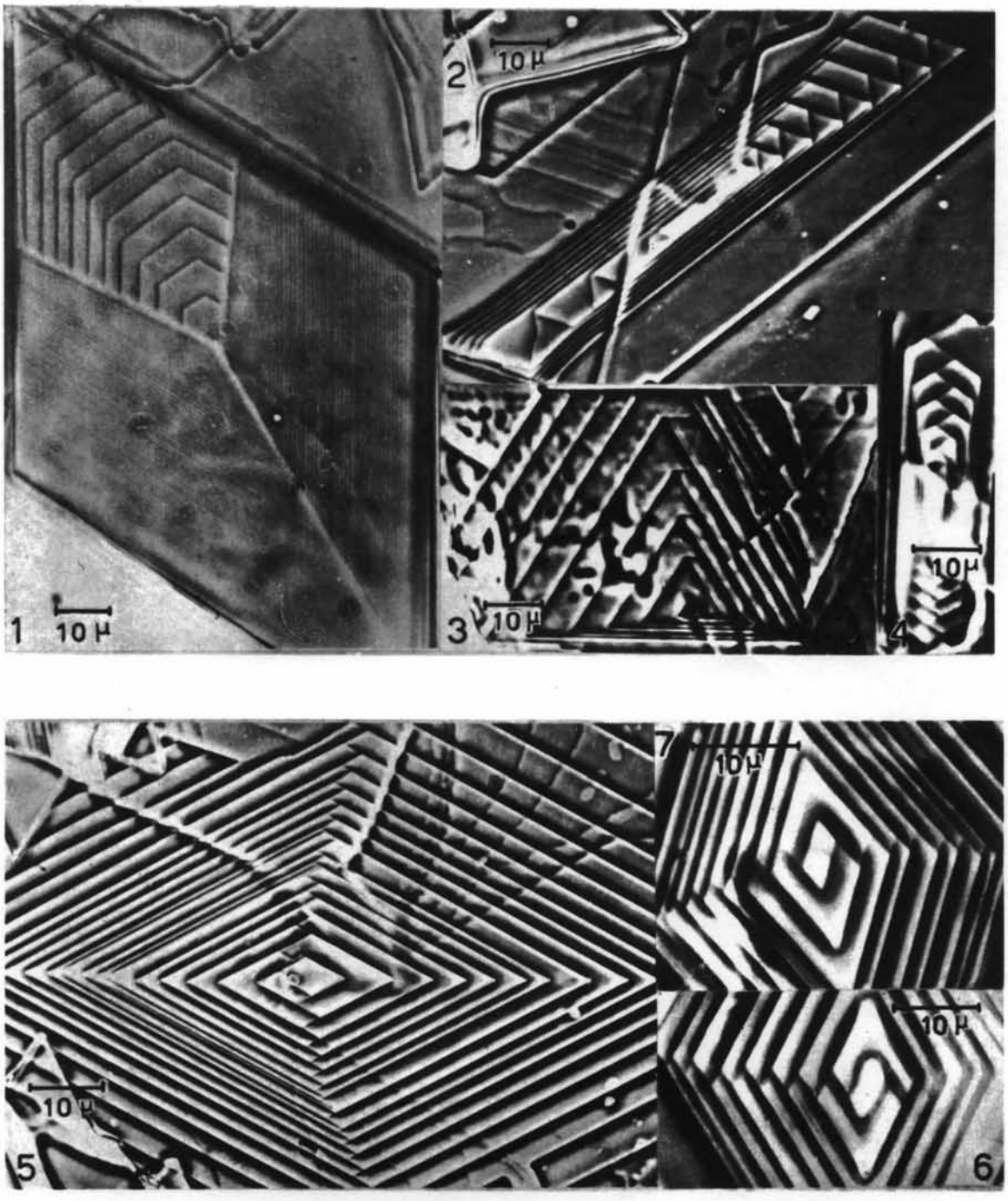

Fig. 1. (1) Normal shape of growth spiral. Steps are bimolecular.
(2) Growth pattern on polytypic crystal; structure symbol: I, I, II, II ($C_{24}H_{49}OH$).
(3) Growth pattern on polytypic crystal; structure symbol: I, III ($C_{22}H_{45}OH$).
(4) Growth pattern on polytypic crystal; structure symbol: I, II ($C_{24}H_{49}OH$).
(5–7) Interlaced spirals on crystals having the stacking sequences (5) I, I, IV, IV ($C_{26}H_{53}OH$); (6) I, IV ($C_{24}H_{49}OH$) and (7) I, I, IV ($C_{24}H_{49}OH$).

[*To face p.* 530

first possibility, as only the second has an observable influence on the growth pattern.

As the allowed relative rotations of two successive bimolecular layers are not symmetry operations for the bimolecular layer itself, which has only a plane of symmetry, four different arrangements, characterized by their relative rotations, are to be considered:

$\varphi=0°$ (normal stacking); $\varphi=60°$; $\varphi=120°$ and $\varphi=180°$.

Frank (private communication) proposed designating these positions (in the same manner as the isomers of di-substituted benzene) by means of the prefixes *ortho*, *meta* and *para*.

3. Polytypism

It has been shown by Frank (1951) that the polytypism of SiC has to be considered as a consequence of his spiral-growth mechanism (Frank, 1949). This mechanism simply assures (except in certain cases; see Part II) the regular repetition of the stacking sequence which was present in the exposed edge of the screw dislocation.

For crystals having in their normal structure differently oriented lamella capable of growing independently, an imperfect dislocation is usually all that is needed to give rise to a polytype, e.g. SiC-6*H* (Frank, 1951) and CdI_2 (Forty, 1952). When this is not the case stacking faults are required. This last condition is fulfilled for the β-form of the *n*-alcohols.

4. Growth features on crystals of the β-form (monoclinic)

4·1. *Polar diagram of the elementary spirals*

The type of growth spiral normally observed on crystals of this modification is shown in Fig. 1(1). The step height, measured by means of multiple-beam interferometry, was found to be equal to d_{001}, so that the steps are bimolecular. We will call this an elementary spiral.

We will now deduce the polar diagram for the growth velocity. This can be done in two ways, which are in fact equivalent:

(i) By considering the spacing between successive windings in a certain sector as a measure of the growth velocity in that sector.

(ii) By measuring the angles $\theta_{j,1}$ and $\theta_{j,2}$ (Fig. 2(*a*); j refers to the sector j). When, putting $\cos\theta_{j,1}=\gamma_j$ and $\cos\theta_{j,2}=\delta_j$, we have immediately:

$$v_j/\delta_j = (v_1/\delta_1)(\gamma_2\gamma_3\ldots\gamma_j/\delta_2\delta_3\ldots\delta_j)\,.$$

This formula gives the relative values of the v_j. The values deduced from Fig. 1(1) are tabulated in Table 1, where the α_i are the directions of the normals to the fronts (Fig. 2). It is clear that the corresponding polar diagram will have five sharp minima in directions which differ very approximately 60° (or 120°) in orientation; they are normal to the close-packed rows of the lattice. It appears further that there is a line of symmetry, so that there are in fact only three different growth velocities; we call them v_a, v_b and v_c and the corresponding minima *a*, *b*, *c*. We then find the polar diagram shown in Fig. 2(*b*).

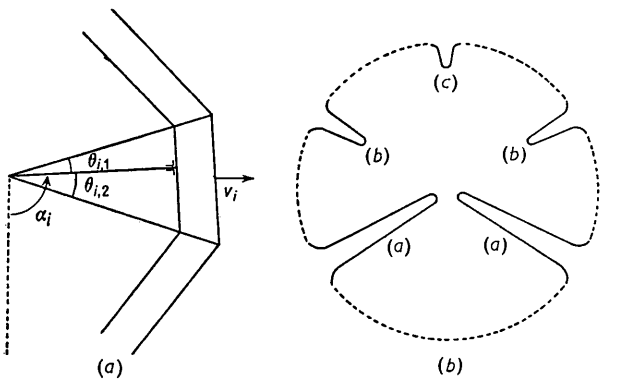

Fig. 2. (*a*) The significance of the angles $\theta_{j,1}$ and $\theta_{i,2}$.
(*b*) Polar diagram for growth velocity of a bimolecular layer under the growth conditions used in our experiments. The polar diagrams of Figs. 3–6 are not drawn to scale; the relative values of the minima only are represented. The diagrams are only intended as an aid in reasoning.

Table 1

Minimum	α_i	v_i
(*c*)	0°	10·1
(*b*)	60° 30′	7·5
(*a*)	119° 30′	1·0
(*a*)	240° 30′	1·0
(*b*)	299° 30′	7·5

It is necessary to insist that this diagram is only intended to facilitate subsequent reasoning and that in fact all we know from observation are the five points of the minima. The rest of the diagram is uncertain. It is, however, possible to make some guesses concerning minima which could develop growth fronts in certain circumstances. One such minimum is to be expected in the direction opposite to (*c*); we would call it (*d*). We can fix only a lower limit for $v_d: v_d \geqslant 2v_a$ (see further § 4·2).

It is further to be kept in mind that the polar diagram so derived is not an invariant of the crystal, but on the contrary varies with growth conditions. In certain cases we found, for example, that (*b*) fronts were not developed, proving that $v_b \geqslant v_a+v_c$ (§ 4·2).

We suppose, however, that the given polar diagram is representative enough to allow the analysis we intend to make.

The symmetry of a polar diagram belongs necessarily to one of the ten plane point groups; in this case it is $1m$ (or D_1; Polya, 1924).

The particular shape of the diagram (i.e. the relative values of the growth velocities) results from at least three different factors: (i) the structure of the growing layer itself, (ii) the field of force of the substrate layer, (iii) the growth conditions.

Owing to the particular structure of the limiting surfaces of a bimolecular layer, the field of force will tend to hexagonal symmetry. The striking anisotropy in growth velocity is, as a consequence, mainly caused by the first factor, i.e. the tilt of the chains. This is confirmed by observations on carboxylic acids. The polar diagrams for crystals of the B and C modifications have also a line of symmetry which is in both cases the trace of the b plane. As the tilt angles (i.e. the angle between the axis of the chain and the normal on $c(001)$) are, however, smaller in the latter case, the anisotropy is less striking.

As a consequence of the approximate hexagonal symmetry of the substrate, a rotation through $\varphi = k\times 60°$ will not seriously influence the shape of the polar diagram. We assume that it remains the same. It will, however, be turned through the same angle as the layer itself, and its orientation as a consequence indicates the orientation of the layer. This last conclusion is important for the analysis of interlaced spirals. It will be noted that after a permitted rotation the minima are in the same directions, or very approximately so, but have different values.

4·2. *Developed growth fronts*

Another question which will arise in the course of our arguments is the following. In which sector will growth fronts be developed for a layer with a polar diagram given as a set of values (α_i, v_i) (corresponding to a perfectly polygonized spiral)? When growth proceeds in a homotetic way and when the growth rate is constant, the condition that a growth front should be developed can be formulated as follows.

If a potential growth front whose rate of advance is v lies between two others with rates of advance v_l and v_r inclined at angles θ_l and θ_r to left and right of it, it will develop as a visible front if, and only if,

$$v < v_c = (v_l \sin \theta_l + v_r \sin \theta_r)/\sin(\theta_l+\theta_r) . \qquad (1)$$

θ values in the present case are multiples of 60° as near as matters. If $\theta_l = \theta_r = 60°$ equation (1) reduces to the very simple form

$$v < v_c = v_l + v_r . \qquad (1')$$

The relation (1′) indicates immediately which growth fronts will be developed for all combinations of minima (a), (b) and (c). We further notice that the minimum (d) will be of no importance in what follows, as it always occurs between two (a) minima, and never has a chance to develop a growth front according to (1′).

4·3. *Interlaced spirals*

We say that a spiral is interlaced when the main growth fronts are connected in certain 'corners' of the spiral by thinner growth fronts; we will call such a 'corner' an 'interlacing'. Interlaced spirals were observed earlier on crystals of silicon carbide (Verma, 1951; Amelinckx, 1951*a*, *b*), cadmium iodide (Forty, 1952) and biotite (Amelinckx, 1952; Amelinckx & Dekeyser, 1952). An explanation of the interlacing mechanism on silicon carbide crystals ($6H$) has been given by Frank (1951).

We now observed three different types of such spirals (Fig. 1 (2, 3 and 5)) on crystals of the n-alcohols containing 22, 24 and 26 carbon atoms.

The origin of the phenomenon is the presence in certain sectors of growth fronts having different growth velocities. A small difference is sufficient to cause the grouping of growth fronts behind the slowest one of the succession in a sector. When the slowest front belongs to a different layer in different sectors interlacing results.

In the present case a relative rotation of $\varphi = k\times 60°$ of two successive layers will bring different minima of the polar diagrams into superposition in the same sector and this will cause interlacing.

We will now formulate in a general way the necessary condition for interlacing. We have to consider on one hand the stacking symmetry (S), on the other hand the plane symmetry of the polar diagram (P). When an element of S (the unit element being excluded of course) works on the polar diagram, different minima will be superposed only if the cyclic point group S is not a subgroup of P.

We suppose here implicitly that S and P are not totally independant. We accept, for example, that when S is $\varphi = k\times 60°$ the minima will enclose angles of 60° and not of 90°.

As the symmetry operators P and S are in practice related to the spatial symmetry of the crystal, it is not astonishing to find that the conditions for polytypism and for interlacing of spirals are in fact the same, and that a direct relation exists between both phenomena. This does not mean, of course, that the occurrence of interlaced spirals is a proof of polytypism (see Part II).

4·4. *Analysis of interlaced spirals*

We will now show how the analysis of interlaced spirals can provide information concerning polytypism. We will summarize the procedure for the special case of the β-form of the n-alcohols, but the method is applicable to other cases.

(i) *Determination of the polar diagram for an elementary layer.*—This has been done in § 4·1. The result is Fig. 2(*b*).

(ii) *Allowed relative rotations of successive layers.*—In our case we found $\varphi = k\times 60°$.

(iii) *Decomposition of the interlaced spiral pattern into elementary spirals.*—This part of the scheme requires some elucidation. The first point is to find out how many spirals, i.e. how many separately growing lamella, are present.

A very useful piece of information is the height of the main steps; when the height of an elementary

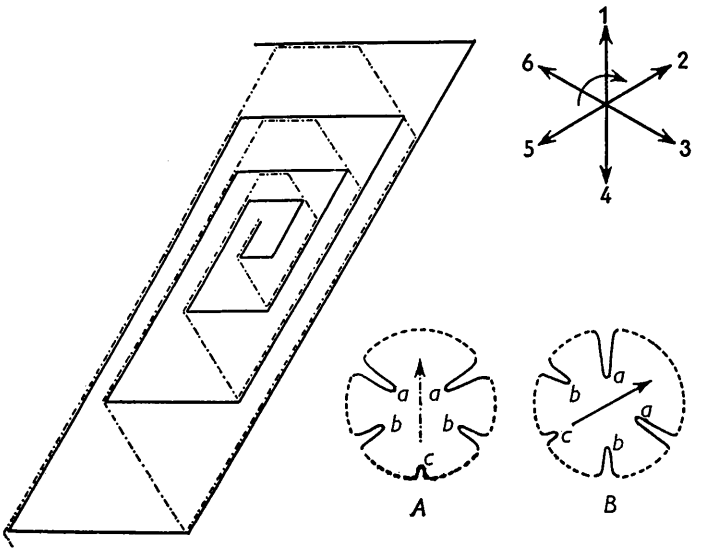

Fig. 3. Decomposition into single spirals of the growth pattern of the *ortho* type.

spiral step is known, the possible number of lamellae follows immediately. Additional difficulties arise when one lamella consists of several elementary layers. We found that in the present case the lamellae were not more than two elementary layers thick, so that no difficulties were met.

We can further find a simple relation between the number (n) of 'interlacings' and the total number (N) of elementary layers. When p_i is the number of layers which advances in the ith 'interlacing' we simply have

$$0 < p_i < N_0; \quad N_0 \leqslant N \tag{1}$$

$$\sum_{i=1}^{n} p_i = kN\,, \tag{2}$$

with

$$k < nN_0/N\,, \tag{3}$$

where k is a whole number. This formula allows us to survey all possible ways of grouping elementary layers into lamella.

Let us consider, for example, the hypothetical case of a hexagonal interlaced spiral with 'interlacings' in three corners 120° apart. We then have $n = 3$. From the geometry alone we know already that more than two spirals are present because, with $N = 2$, relations (1), (2) and (3) cannot be satisfied. We can generalize: *when n is odd the pattern is composed of more than two spirals.* Suppose now $N = 3$; then relations (1) and (2) reduce the number of possibilities which have to be considered to two:

$$p_i = p_2 = p_3 = 1 \quad \text{and} \quad p_1 = p_2 = p_3 = 2\,.$$

The knowledge of the heights of the advancing steps will allow us to decide between both solutions.

* The line drawing of Fig. 3 was made from Fig. 1(2) (which represents a pattern of the same type) because of the better visibility.

We will summarize now the kind of reasoning that has to be made to decompose the spiral (type 1) shown in Figs. 1(4) and 3.* It was found that the step height is four projected chain lengths, i.e. two bimolecular layers. The number of lamellae (bimolecular layers) in a main front is consequently two. Consider now sector 1 and call the upper lammella A and the lower one B; i.e. the composition is A over B. Going to sector 2, part of the growth front (A) retracts; B on the other hand advances and joins the lower A front; the composition of the main front thus becomes B over A. Passing from sector 2 to sector 3, B retracts again and the composition becomes A over B. In sector 4 nothing changes (composition A over B), but A does not always develop a growth front. Going from 4 to 5 the lower lamella is again A, whilst B does not always develop a growth front. Going to sector 6 nothing changes, but, passing again to sector 1, A joins the lower lamella B and the composition becomes again A over B, i.e. the same as at the start.

The principle used is simply that only the bottom lamella of a front is capable of advancing whilst the upper lamella is the only one that can retract. The result of this reasoning is represented schematically in Table 2.

Table 2

Sector	1	2	3	4	5	6	1
Composition	A	(B)	A	(A)	(B)	B	A
	B	A	B	B	A	A	B

(Fronts not developed are between brackets.)

We have also represented graphically the decomposition of the interlaced spiral in its component spirals (Fig. 3).

(iv) *Determination of the orientation of the lamellae.*— It is assumed that as a first approximation the lower

lamella of a front in a given sector is rate determining. When no change in composition has taken place when entering a sector, one can, however, only conclude that the lower lamella in that sector is not growing faster than the upper one. We can express this in the following set of inequalities (${}^1v_A$ means the growth velocity of A in sector 1):

$$ {}^1v_B < {}^1v_A \quad (1), \qquad {}^4v_B \leqslant {}^4v_A \quad (4), $$
$$ {}^2v_A < {}^2v_B \quad (2), \qquad {}^5v_A < {}^5v_B \quad (5), $$
$$ {}^3v_B < {}^3v_A \quad (3), \qquad {}^6v_A \leqslant {}^6v_B \quad (6). $$

We now have to superpose the two polar diagrams of A and B in such orientations that all the relations (1) ... (6) are satisfied. We will characterize the positions by means of roman cyphers, e.g. orientation II means that the polar diagram is oriented so that the arrow points to sector 2. The shortest way of proceeding is to fix first the position of one lamella. This can sometimes be achieved by taking into account that the deepest minimum (a) must fall in the sector where the spacing is the smallest. This fixes the position of A: I. Relations (1) ... (6) now allow us to exclude certain orientations for B. The result of the elimination process is summarized in Table 3.

Table 3

Relation	Excluded position for B
(1)	I
(2)	I, III
(3)	III, V, VI
(4)	—
(5)	III, IV, VI
(6)	—

It appears that only II is left as a possible orientation for B. We can describe the probable structure by means of the symbol I, II (I for A, II for B), i.e. the *ortho*-structure.

(v) *Control of proposed structure.*—We will now show that the proposed structure explains the observed growth pattern. To facilitate the reasoning we have drawn the two polar diagrams in their correct orientation with respect to the pattern (Fig. 3).

In sector 1 it is clear that the growth velocity of B has the deepest minimum; this means that B will be the slowest growing lamella and hence the underneath one. The composition of the main fronts is thus A over B. In sector 2, however, the deepest minimum refers to lamella A. The growth front B will as a consequence join the lower layer A and build up a front B over A. In sector 3, B is again the slowest growing layer and the growth fronts will thus change in composition; it becomes A over B. In sector 4 lamella B is still the slowest one and as a consequence nothing will change. In 5, A becomes again slow, so the composition changes between 4 and 5. In 6, A remains slow; the composition of the front is B over A. Returning now to sector 1 the composition has again to change as now B becomes slow. We thus arrive in 1 with the same composition as at the start. It will be evident that the composition is correct in every sector and that interlacing takes place in accordance with observation.

We have given the reasoning in some length for this first case; this makes it possible to summarize for the other cases.

4·5. *Type* 2 (Figs. 1(3) and 4)

Composition of growth fronts.—The composition scheme is given in Fig. 4. The following inequalities can now be derived:

$$ {}^2v_A \leqslant {}^2v_B \ (1), \quad {}^4v_B < {}^4v_A \ (2), \quad {}^6v_A < {}^6v_B \ (3). $$

These, however, are not sufficient to derive a unique hypothesis for the orientations of the successive layers.

From the fact that no growth fronts are developed for B in sectors 1, 3 and 5 we can, however, conclude that the growth velocity in these sectors certainly exceeds the maximum value allowed for the formation of a front. The least restricting hypothesis is now that the two adjacent minima are (a)-minima; we then have, without loss of generality, (using equation 4·2. (1′))

$$ {}^1v_B > v_a \ (4), \quad {}^3v_B > v_a \ (5), \quad {}^5v_B > v_a \ (6). $$

Using now the relations (1), (2), (3) and (4), (5), (6) we can first derive the position for A and further we can exclude positions for B with respect to A in the same way as above. The result of the elimination is that B can only have the orientation III. The hypothetical structure is thus I, III, i.e. the *meta*-structure.

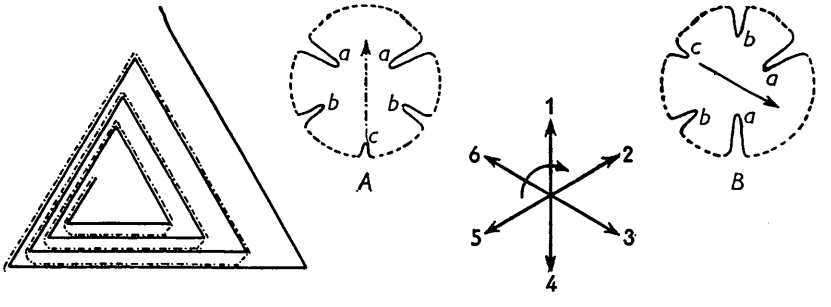

Fig. 4. Decomposition into single spirals of the growth pattern of the *meta* type.

It is now easy, using the polar diagrams of Fig. 4, to verify that this hypothesis is consistent with the growth pattern.

4·6. *Type* 3 (Figs. 1(6) and 5)

(i) *Composition of growth fronts.*—The scheme is given in Fig. 5.

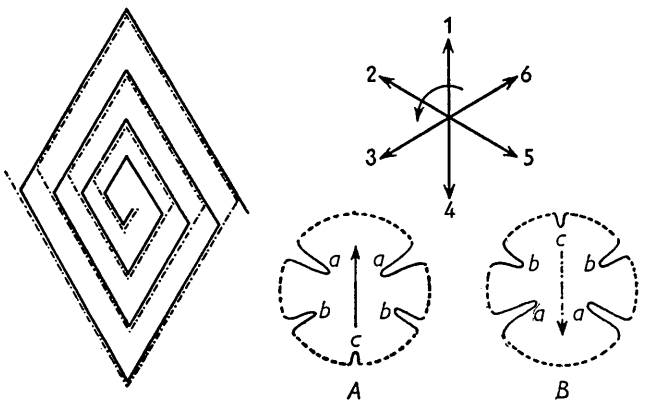

Fig. 5. Decomposition into single spirals of the growth pattern of the *para* type.

(ii) *Determination of the orientation of the polar diagrams.*—We have the following set of inequalities:

$$^2v_A \leqslant {}^2v_B \ (1), \qquad {}^3v_B < {}^3v_A \ (3),$$
$$^6v_A < {}^6v_B \ (2), \qquad {}^5v_B \leqslant {}^5v_A \ (4).$$

Fixing first the position for A, i.e. I, and eliminating positions for B by the use of (1), ..., (5) leaves IV as the only possible orientation for B.

The only remaining hypothesis consistent with observation is thus the structure I, IV, i.e. the *para*-structure.

It is easy to verify that this hypothesis gives correct interlacing and spacing.

4·7. *Missing growth fronts*

The reason for the missing of growth fronts in certain sectors is immediately clear from formula (1′):

(i) *Type* 1.—A and B do not develop fronts respectively in 4 and 5 because a minimum (c) cannot develop a growth front between a minimum (a) and a minimum (b).

(ii) *Type* 2.—A and B have no fronts respectively in 1 and in 1, 3 and 5 because the minimum (b) cannot develop growth fronts between two minima (a).

(iii) *Type* 3.—A and B have no fronts respectively in 1 and 4 because the minimum (c) cannot develop a front between two minima (a).

It will further be found that certain details of the observations are *not* explained by the present simple theory. In Fig. 1(4), for example, the spacings for a fronts and b fronts are not in the ratio 1:7·5, as they ought to be; whilst in Fig. 1(2) the a fronts at the 'end' of the figure travel much faster than the a fronts at the 'sides'. In Fig. 1(3) the three a fronts also have unequal spacing. More discrepancies can be found. Some of the reasons responsible for them are: (1) The influence of the substrate on the polar diagram. In reality the substrate has not perfect hexagonal symmetry. (2) The influence of growth conditions on the polar diagram. In the analysis of an interlaced spiral one ought to use the polar diagram deduced from a spiral grown in the same circumstances, which

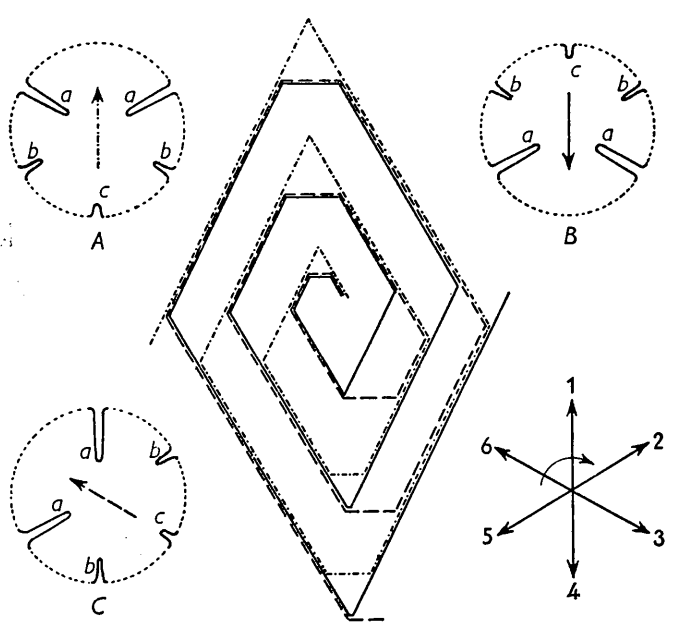

Fig. 6. Decomposition into single spirals of the growth pattern on complicated polytype.

is not always possible. (3) Unsymmetrical environment of the crystal in the solution. (4) The rate of advance of steps containing differently tilted molecules may not be simply determined by the rate of advance of the bottom layer.

We think, however, that the main conclusion is unaffected by these considerations.

Even an inversion of the relative values of v_b and v_c, making v_c slightly smaller than v_b, would not affect our conclusions, provided they both remain much larger than v_a. It thus appears that, at least in this case, the determination of a stacking sequence is not very sensitive to details of the postulated polar diagram. This will probably be so in every case where very pronounced minima (our (*a*) minima) are present; only the deepest minima determine the orientation of the layer.

4·8. *Conclusions concerning the structure of crystals of the β modification*

We have deduced from the growth patterns *alone* that crystals of the form β can present different stacking sequences. In particular, it has been proved that successive bimolecular layers can have orientation differences of $\varphi = k \times 60°$. For two layers there are only four different growth patterns, because the patterns corresponding to $\varphi = 240°$ and $\varphi = 300°$ are mirror images of those corresponding to $\varphi = 120°$ and $\varphi = 60°$ respectively.

As the acute angle χ of the lozenge is not exactly 60°, the CH_3 groups are only approximately close-packed, and therefore the six positions $\varphi = k \times 60°$ are not energetically equivalent. The normal position is of course highly favoured. The *para*-position causes practically no misfit (even when $\chi \neq 60°$) whereas the *ortho*- and *meta*-positions cause an equal degree of misfit. It is therefore to be expected that the probabilities for the different orientations are unequal. This is in fact found; for a certain number of polytypic crystals, chosen at random, we noted the following frequencies:

Type	Number of times observed
Ortho	2
Meta	2
Para	13

No difference in growth pattern was noticed for the three alcohols which were studied.

4·9. *More complicated interlaced spirals*

The preceding speculations suggest that more complicated stacking sequences might occur; this is in fact so and one example is shown in Fig. 6, which gives at the same time the composition scheme.

Reasoning along the same lines as above, it can be shown that two solutions are consistent with the observed pattern: they are respectively I, IV, VI and I, II, VI (I for *A*, II for *B*, VI for *C*).

In Fig. 6 the three polar diagrams are represented in their correct orientation according to the first solution; it is easy to verify that correct composition and interlacing is obtained. The missing growth fronts are explained in the same way as above.

The second solution also satisfies. The first solution is, however, more probable than the second because of the greater probability of a rotation $\varphi = 180°$. The crystal on which this pattern was observed is in each case a triclinic polytype with a d_{001} equal to the projected length of six molecules.

4·10. *Other polytypes*

Other crystals were found which contained more than two bimolecular layers in the unit cell.

Fig. 1(2) shows a growth pattern of the *ortho* type, but both growth lamellae are two bimolecular layers thick; the structure symbol is consequently I, I, II, II. Fig. 1(5) and Fig. 1(7) show two growth patterns of the *para* type. It is clear that the steps are not elementary; in one case (Fig. 1(5)) the structure symbol is I, I, IV, IV; in the other (Fig. 1(7)) the steps are unequal and the structure symbol is I, I, IV.

Table 4 summarizes the characteristics of a number of observed polytypes.

Table 4

Symmetry	Structure symbol	Fig.	Number of bimolecular layers in unit cell
Monoclinic	I	1(1)	1
Monoclinic	I, II	1(4)	2
Monoclinic	I, III	1(3)	2
Orthorhombic	I, IV	1(6)	2
Monoclinic	I, I, IV	1(7)	3
Triclinic	I, IV, VI (or I, II, VI)		3
Orthorhombic	I, I, IV, IV	1(5)	4
Monoclinic	I, I, II, II	1(2)	4

5. Origin of polytypism

In the present case polytypism cannot be due to imperfect dislocations. This will be shown in Part II, where we will also prove that polytypism (or disorder) due to the 'up-side-down' position of molecules does not occur in *n*-alcohols.

The occurrence of the polytypes described can be explained only by accepting the existence of stacking faults of a well defined type, i.e. which can be described in terms of relative rotations of successive layers through angles $\varphi = k \times 60°$. We see two ways in which these stacking faults can be generated: (1) by deposition of a two dimensional nucleus in a wrong orientation; (2) by contact, during growth, of two layers having the correct orientation difference (or approximately so).

This last possibility arises as a consequence of the particular way of preparing the crystals. They grow by slow evaporation of the solvent on an object glass. Suppose that two elementary layers (bimolecular) meet with an orientation difference which is approximately one of the allowed values. A layer which is subsequently deposited in correct position on one of the first layers will eventually grow over the boundary and will impose the same inclination of the chains also on the second crystal where the tilt of the chains is now different from the one in the first layer. Growth around a dislocation in such a crystal will give rise to a polytypic crystal if the Burgers vector is large enough to expose a layer of both orientations.

I wish to thank Prof. Dr W. Dekeyser for his interest in these observations and Prof. F. C. Frank for valuable criticism. This work is part of a research program supported by I.R.S.I.A. (Institut pour l'encouragement de la Recherche Scientifique dans l'Industrie et l'Agriculture); Comité pour l'étude de l'Etat Solide (Brussels).

References

AMELINCKX, S. (1951*a*). *J. Chim. phys.* **48**, 475.
AMELINCKX, S. (1951*b*). *Nature, Lond.* **168**, 431.
AMELINCKX, S. (1952). *C. R. Acad. Sci., Paris*, **234**, 971.
AMELINCKX, S. (1953*a*). *Naturwissenschaften*, **40**, 620.
AMELINCKX, S. (1953*b*). *C. R. Acad. Sci., Paris*, **237**, 1726.
AMELINCKX, S. (1954). *Naturwissenschaften*, **41**, 356.
AMELINCKX, S. & DEKEYSER, W. (1952). *Comptes Rendus de la 19e Session du Congrès Géologique international*, **18**, 9.
ANDERSON, N. G. & DAWSON, I. M. (1953). *Proc. Roy. Soc.* A, **218**, 255.
DAWSON, I. M. (1952). *Proc. Roy. Soc.* A, **214**, 72.
DAWSON, I. M. & VAND, V. (1951). *Proc. Roy. Soc.* A, **206**, 555.
FORTY, A. J. (1952). *Phil. Mag.* (7), **43**, 72.
FRANK, F. C. (1949). *Disc. Faraday Soc.* **5**, 48.
FRANK, F. C. (1951). *Phil. Mag.* (7), **42**, 1014.
POLYA, G. (1924). *Z. Kristallogr.* **60**, 278.
VERMA, A. R. (1951). *Phil. Mag.* (7), **42**, 1005.
VERMA, A. R. & REYNOLDS, P. M. (1953). *Proc. Phys. Soc.* B, **66**, 414.
WILSON, P. A. & OTT, E. (1934). *J. Chem. Phys.* **2**, 231.

Acta Cryst. (1955). **8**, 537

La Méthode Statistique en Cristallographie. I

PAR E. F. BERTAUT

Laboratoire d'Électrostatique et de Physique du Métal, Institut Fourier, Place du Doyen Gosse, Grenoble, Isère, France

(*Reçu le* 12 *novembre* 1954)

Two general theorems are enunciated on the probability of the value of certain functions. From these we deduce a concise mathematical formulation of the statistics of structure factors and of the joint probability of structure factors. By means of a characteristic function we have systematized the correlation between structure factors and have extended the results of Hauptman and Karle.

Introduction et plan

Les méthodes statistiques en cristallographie, inaugurées par Wilson (1949), continuées par Hauptman & Karle (1954), Karle & Hauptman (1952, 1953), Rogers (1950), Luzzati (1953), Cochran (1954), Woolfson (1954), Vand & Pepinsky (1953) et tant d'autres, ont pris une telle extension qu'il nous a paru utile de rechercher une base de départ aussi générale que possible, jointe à une formulation mathématique aussi simple que possible.

Nous avons été amené ainsi à démontrer dans la partie I deux théorèmes très généraux de la théorie des probabilités qui d'ailleurs peuvent s'appliquer à bien d'autres sciences que la cristallographie. Le premier traite de la probabilité de la valeur d'une fonction, le deuxième de la probabilité composée de valeurs de plusieurs fonctions (I–2°). Dotée des résultats concis de la partie I, la méthode devient plus claire et plus directe que celle de Hauptman & Karle (1954) tout en aboutissant, sans aucune hypothèse supplémentaire, à des résultats essentiellement équivalents.

Dans la partie II la méthode est appliquée à la statistique générale des facteurs de structure (II–1°). On y traite également de la relation avec la statistique de Wilson (II–2°), de l'influence des symétries sur les réflexions générales (II–3°*a*) et spéciales (II–3°*b*) et de la valeur moyenne d'une puissance $|F|^p$ d'un facteur de structure où le résultat est particulièrement simple (II–4°).

La partie III considère la probabilité composée, correspondant à un très grand nombre de facteurs de structure. Notre méthode apparaît alors traduire analytiquement les idées de Vand (1954) (III–1°). Grâce à l'introduction d'une fonction caractéristique (III–2° et I–4°), le calcul de la probabilité composée,